Combined Predictive Research on Timber Building Internal Defects

Li-Hong Chang [a, c*] , Wei Qian [b, c] , Jian Dai [b, c] , Xin Li [b, c], and Jun Ma [c]

a: College of Architecture and Civil Engineering, Beijing University of Technology, Beijing, 100124, China;
b: College of Architecture and Urban Planning, Beijing University of Technology, Beijing, 100124, China;
c: Beijing Engineering Research Center of Historic Buildings Protection, Beijing, 100124, China

***Abstract* - In order to study the internal damage of ancient architecture wood members, in this paper the stress wave and impedance instruments were applied to test Pinus tabulaeformis and elm specimens with different damage types and internal defect areas. Combined prediction was also conducted on their internal defects on the basis of the Shapley value. The results showed that when the internal damage was holes, stress waves could obtain the two-dimensional image of the test section quickly and determine the damage positions, sizes, and types. When internal wood was damaged by insects, the actual defect was proportional to the error value of the absolute error. Impedance instrument accurately determined defect positions and damage types of a single path. The impedance instrument test results were more accurate with smaller internal defect areas. According to the Shapley value, the weight function of the stress wave and impedance instrument were confirmed through distributing the total error values of the two testing methods so that the combined predictive model was constructed. The combined prediction error value more accurate than single test results. The research results are useful to aim preventive protection of ancient buildings, and can provide effective data support for practical engineering repair and reinforcement of buildings because the research adopted the detective method of quantitative analysis instead of qualitative analysis.**

Keywords - Ancient building; Timber structure; Internal defects; Combined predictive

I. INTRODUCTION

With a history of thousands of years, 70% of Chinese ancient buildings by investigation are made of wood. The timber frame has many advantages, for example structure is very light and comparatively flexible, beautiful shape, high machinability, replaceable components and better anti-seismic performance, etc [1,2]. Though it is a biological material, it also brings with it anisotropy at the same time [3]. It is vulnerable to degradation internally or externally due to factors such as temperature, humidity, integrated environment, and tenure of use [4,5]. Internal degradation cannot be judged from appearance and degradation area continues to increase with the passage of time [5,6], which results in low utilization rate of resources, and even irrecoverable losses. Traditional knocking or saw cutting method will destroy the woods' integrity to some extent. Also, testing results will largely depend on human experience and it lacks the ability to be expressed quantitatively [7]. Therefore, a quick and precise testing method without destroying the premise of lumber itself is necessary.

In recent years, scholars have used various research methods such as X-ray scanning, stress wave, impedance instrument, and ultrasonic wave to test wood internal defects [8, 9, 10, 11]. It has been found that the convenience, security, and testing methods for the visualization of stress wave and impedance instrument made them more suitable for field application [12, 13]. However, these two methods have their own advantages and disadvantages, giving rise to different testing results. Consequently, from the perspective of protect excellently the old buildings and other historic and cultural heritages, what urgently needs to be solved is the qualitative and combined predictive quantitative research on wood internal defects testing results.

In this report, through simulating common internal holes and defects caused by insects and using non-destructive testing methods of stress wave and impedance instrument, comprehensive analysis was conducted on how two-dimensional detection images and areas with different damaged sections reflected wood internal defects and the sensitivity of data collection. The Shapley value weight function distribution method was used to determine the weight function of internal defects prediction model of the tests in order to construct non-destructive testing combined prediction model[14,15], complete combined prediction for wood internal defects, reduce error value of single tests, improve overall accuracy, acquire new practical method for wood non-destructive testing internal defects prediction, and provide strong data support for lumber disease. All of these are conducive to ancient building future health and safety

evaluation as well as protection and effective utilization of architecture inheritance.

II. MATERIALS AND METHODS

A. Field Investigation

By field investigation the ancient buildings in Northern China (Beijing, Shan'xi and Henan) and Southern China (Anhui, Hunan and Guangxi) (Fig.1).

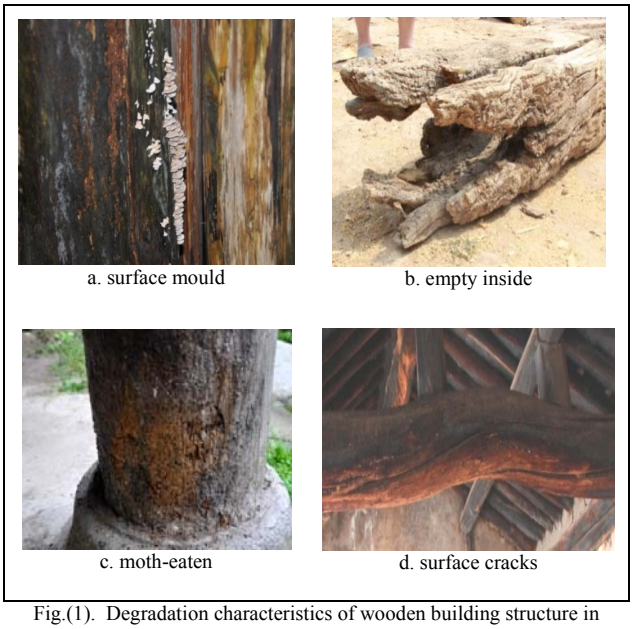

a. surface mould b. empty inside c. moth-eaten d. surface cracks

Fig.(1). Degradation characteristics of wooden building structure in China

Through the complex network analysis, found the holes or decay have bigger relevance with other damage types. And inner holes and decay by external observation is not easy to judge. Holes and decay simulation test was carried out on the specimen.

B. Materials

The experimental material used in this study was the column disassembled from Beijing ancient building repair project with same internal material and no obvious decay or defect. The tree species were identified as Pinus tabulaeformis and Elm (Fig.2), both of which had a moisture content below 15% by debugging. The timber was lined and sawed after its original state was analyzed. The height of the two test specimens were 100 mm. A holes and moth-eaten simulation test was carried out on the specimen, which was detailed in Table 1. This test employed a reverse testing method, and according to sizes, wood internal defects of BYS-1, BYS-4, XYM-1, and XYM-4 were continuously extended artificially. Defect areas (S) accounted for S /9, S /7, S /5, S/3 and S/2 of test section respectively.

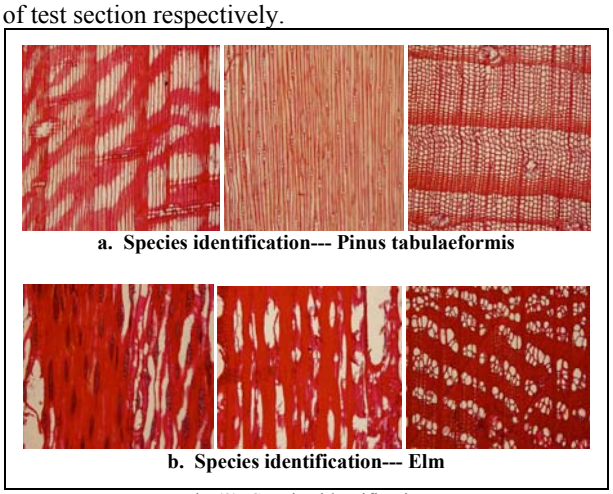

a. Species identification--- Pinus tabulaeformis

b. Species identification--- Elm

Fig.(2). Species identification

TABLE I. TEST SPECIMEN

Number	BYS-1	BYS-4	XYM-1	XYM-4
Species	Pinus tabulaeformis	Pinus tabulaeformis	Elm	Elm
C/mm	970	910.30	1100.00	1120.60
H/mm	100	100	100	100
Moisture Content %	14.2	12.5	10.7	10.9
Simulation types	Holes in centre	Moth-eaten in centre	Holes in centre	Moth-eaten in centre
Detecting Height/mm	50	50	50	50

C. Methods

Hungary FAKOPP ten probe stress wave was adopted to collect data from the specimen with internal defects. The internal parts of specimen produced stress wave when vibrating and the travel time of internal section under different paths was calculated by matrix and reconstruction. Therefore, the statistics were transformed into an intuitive two-dimensional image and consequently, wood internal defects could be distinguished in line with different colors [16]. The positions, sizes, and areas of internal defects were analyzed through ArborSonic 3D software.

Germany IML-750 impedance instrument was introduced to collect data from specimen simulating wood internal defects. The revolving speed was 5000 r/min and the needle speed was 200 cm/min. Different resistances encountered by the probe going forward formed a relative resistance value of this path and internal defects two-dimensional images. The testing value reflected internal defects under the needle path. Abscissa of the image indicated micro-probe path length; therefore, the

categories, positions, and areas of wood internal defects were determined on the basis of the testing image.

The images and areas of the testing results of stress wave and impedance instrument were analyzed to determine the nature of wood internal defects. At the same time, wood internal defects area values tested by stress wave and impedance were compared in order to set up a combined predictive model for calculating and evaluating internal defects area, thus improving effective utilization of the ancient building.

III. RESULTS AND DISCUSSION

A. Two-dimensional Images Contrastive Analysis

Internal holes and moth-eaten simulation test on the specimens BYS-1, BYS-4,XYM-1, and XYM-4 was carried out by FAKOPP stress wave and IML impedance instrument. For example, when the internal defects was holes in BYS-1 and BYS-4, whose internal defects accounted for S /7 of sectional area, the central part of the stress wave two-dimensional image turned from green to blue and red. This reflected that internal defects were located at the center of the specimen and that it was round, which was determined by internal holes. This shows that wood internal part is damaged thoroughly when defects are holes and stress wave data collection is sensitive. It also shows that the two-dimensional image can identify the sizes and positions of internal defects more accurately (Fig. 3a). However, the stress wave two-dimensional image of BYS-4 revealed that the central part turned into yellow from green and internal defects were roughly located in the center. Therefore, neither the shape or type of defects could be confirmed, which illustrated that when wood internal defects of the same species is caused by insects and the path is free from complete damage for lignin connecting in degradation places, stress wave during transmission sees it as sound wood. This lead to a weak identification for moth-eaten area by the two-dimensional image (Fig. 3b).

Impedance instrument probe selected the radial and tangential testing section (point 1-6 ; 3-8 ; 5-10) and crossed through defective parts. The two-dimensional image could accurately reflect the positions and lengths of defects. It has been found, by comparing the two-dimensional testing image results of stress wave and impedance instrument (Fig.4) that when wood internal hole diameter was greater than 9 cm, resistance was lost and probe was shaken easily. Therefore, in a deviating testing path, the probe would simultaneously come back to protect itself if there was no resistance for a long time; hence, when BYS-1 Pinus tabulaeformis S/7 S specimen was detected by impedance instrument, the probe pushed to get through the holes. On the contrary, when insects caused internal holes, the probe experienced an irregular relative resistance value.

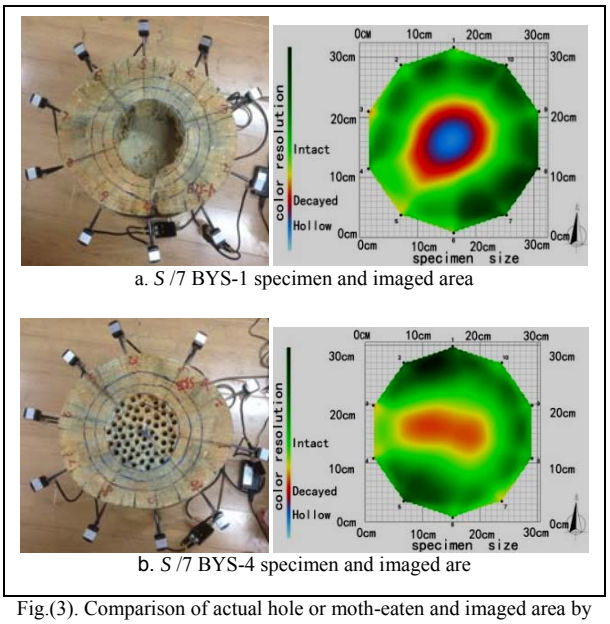

a. *S* /7 BYS-1 specimen and imaged area

b. *S* /7 BYS-4 specimen and imaged are

Fig.(3). Comparison of actual hole or moth-eaten and imaged area by stress waves

There was a great difference between the values of peaks and troughs and the internal defects were defined as moth-eaten by their continuity. When specimen BYS-4 reached S/7 of the section, point 1-6 impedance instrument path was abnormal in the central part (Fig.4a). The testing result was similar to that of stress wave in the same path and the length was 115 mm (Fig.4b). However, impedance instrument could have just reflected internal defects in single path instead of the whole section defects.

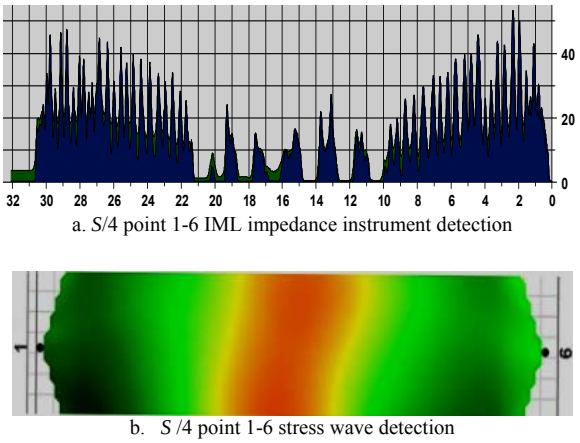

a. *S*/4 point 1-6 IML impedance instrument detection

b. *S* /4 point 1-6 stress wave detection

Fig.(4). The contrast of stress wave detection and IML impedance instrument detection

By comparing two-dimensional images of the above two testing methods, it can be concluded that stress wave non-destructive testing method can make preliminary intuitive judgment on positions as well as wood internal

section defects degrees. However, the results cannot determine the types and the boundaries of the defects as clearly. Impedance instrument can accurately decide the defects length and type in single path, but there are limitations on the number of probes into wood and judgment on the whole section is poor.

B. Internal Defects Image Area Contrastive Analysis

Specimens of BYS-1, BYS-4, XYM-1 and XYM-4 were simulated artificially for different internal defects areas and the actual defects area was S0. The wood was detected by stress wave and impedance instrument. The damage percentage and area (S1) of the whole cross section were obtained through analysis by stress wave ArborSonic 3D software. Impedance instrument was for single path detection, after circle center radical and two-chordwise (point 1-6 ; 3-8 ; 5-10) probing into the tested wood, the positions and sizes of wood internal damages in single path were explicit. The three paths intersected, forming different damage lengths (ri, ri+1, …rn). Adjacent deteriorated points were linked together to simulate several triangles with various areas, so as the whole tested section damaged area (S2) was

$$S = \sum_{i=1}^{n-1} \times r_i \times r_{i+1} \times \sin\frac{360^\circ}{n} \qquad (1)$$

In this equation: S is the overall damaged area of the tested section, n is the number of damaged edges, and r1 is the damaged length of r1.

According to Table 2, divergence exists among testing results of the specimens with different damaged areas as detected by stress wave and impedance instrument. The absolute error (M1) of stress wave testing results can reach a maximum value 40.35 cm2. When internal defects area is detected by impedance instrument, the internal defects are small and the probe can conduct detection in line with the regular test path. However, when internal defects unceasingly expand, the probe path will lose its direction because of the sudden drop of resistance value, leading to unstable swings. Moreover, the inserting and rotational speed of the probe remains unchanged, so the probe can be easily broken off or deviate from the expected testing path, causing that internal defects area (S0) to be proportional to M2.

TABLE II. TESTING RESULTS

Test Specimen	Defect types	Holes Proportion	S_0 /cm^2	S_1 /cm^2	S_2 /cm^2	S_3 /cm^2	M_1 /cm^2	M_2 /cm^2	M_3 /cm^2	Prediction error		
										Q_1/%	Q_2/%	Q_3/%
XYS-1	Holes	*S* /9	83.28	122.43	51.53	101.24	39.15	31.75	17.96	47.01	38.12	21.57
		S /7	107.07	127.41	88.76	115.86	20.34	18.31	8.79	19.00	17.10	8.21
		S /5	149.90	164.89	113.97	149.67	14.99	35.93	2.10	10.00	23.97	0.15
		S /3	249.84	262.33	215.09	248.21	12.49	34.75	1.63	5.00	13.91	0.65
		S /2	374.76	39.78	337.64	376.30	18.02	37.12	1.54	4.81	9.91	0.41
Average value							21.00	31.57	6.40	17.16	20.60	6.20
XYS-4	Moth	*S* /9	73.76	83.02	67.35	76.35	9.26	6.02	0.29	12.55	12.23	0.16
		S /7	94.83	115.99	73.24	50.64	21.16	21.59	7.22	1.94	12.28	7.61
		S /5	132.77	129.68	116.68	124.00	3.09	16.09	9.59	2.32	12.12	7.22
		S /3	221.28	248.49	199.50	108.49	27.21	21.78	27.29	14.82	9.84	12.33
		S /2	331.92	352.75	304.81	331.82	20.83	27.11	47.64	17.53	11.18	14.35
Average value							16.31	18.52	18.41	9.83	11.53	8.33
XYM-1	Holes	*S* /9	107.09	154.21	77.68	118.46	47.12	29.41	11.37	44.00	27.46	10.62
		S /7	137.69	173.49	104.99	141.49	35.80	32.70	3.80	26.00	23.75	2.76
		S /5	192.76	221.68	144.82	185.78	28.92	47.94	6.98	15.00	24.87	3.62
		S /3	321.27	342.34	280.38	313.40	21.07	40.89	1.12	6.56	12.72	2.45
		S /2	481.91	462.63	420.31	466.22	19.28	11.60	15.69	4.00	12.78	3.26
Average value							30.44	32.51	7.79	19.11	20.32	4.54
XYM-4	Moth	*S* /9	112.61	111.04	104.18	114.26	15.43	8.43	1.65	13.70	7.49	1.47
		S /7	144.21	131.23	129.20	130.06	12.98	15.01	14.15	9.00	10.41	9.81
		S /5	201.89	211.98	185.47	196.67	10.09	16.42	5.22	5.00	8.13	2.59
		S /3	336.48	312.93	313.62	313.33	23.55	22.86	23.15	7.00	6.79	6.88
		S /2	504.73	464.38	479.78	473.27	40.35	24.95	31.46	8.00	4.94	6.23
Average value							20.48	17.53	15.13	8.54	7.55	5.40

C. Shapley Value Combined Prediction Damage Model Analysis

There are advantages and disadvantages in applying stress wave and impedance instrument to testing the wood with different defect types and areas. Also, the composite model is obtained through comprehensive analysis on testing results. Assuming that there are N different methods to test the same wood defects, the combined predictive model of N testing results is:

$$f_t = \sum_{i=1}^{N} k_i f_{it} \tag{2}$$

In this equation, ft is the predicted value of internal damage combined predicted model; fit is the predicted value of the i kind of internal damage detection; i=1,2,…, ; ki is the weight function of the i kind of internal damage detection, i=1,2,…, ; and $\sum_{i=1}^{N} k_i = 1$.

D. The Optimal Weight Function Calculating Method Based on Shapley Value

Wood internal nondestructive testing method produces combined prediction overall error, which is separated by the Shapley value weight function method to determine the weight function of testing value. Assuming that there are n kinds of internal defect testing methods to conduct combined prediction, then I={1,2, … }. For any I subset pq (any combination among n kind of methods), E(p) and E(q) signify internal defects testing error. The definition is read as follows:

1) For any I subset pq, there will always be E(p)+E(q)≥E(p∪q)

2) ; xi demonstrates the error value of the i method when cooperation is ultimately shared (xi ≤E(i))

3) E(n), the overall error prod uced in combined internal defect prediction by n kind of nondestructive testing methods, will be entirely separated among n kind of prediction methods:

$$E(n) = \sum_{i \in n} x_i$$

Assuming that Ei is the average value of the i nondestructive testing method error absolute value and that E is the overall value of combined prediction, equation (3) is:

$$E_i = \frac{1}{m} \sum_{j=1}^{m} \left| e_{ij} \right|, \quad (i = 1,2,\cdots n);$$

$$E = \frac{1}{n} \sum_{i=1}^{n} E_i \tag{3}$$

In this equation, m is the number of specimen and eij is the j specimen error absolute value of the nondestructive testing method. The weight function distribution equation of the Shapley value algorithm is

$$E_t' = \sum_{p_i \in p} w(|p|)[E(P - \{i\})] \tag{4}$$

$$w|p| = \frac{(n - |p|)!(|p| - 1)!}{n!} \tag{5}$$

In this equation: w |p| is the weighting factor, indicating the combined marginal contribution that i should bear in nondestructive test; P-{i} is the eliminating model i in combination; i is a certain testing prediction model in combined prediction; E'i is a shared error of i predictive model, namely, the Shapley value; p is any subset of i; and |p| is the number of prediction model in combination.

From equations (4) and (5), the weight function calculating equation of every prediction method in combined prediction can be known as

$$w_i = \frac{1}{n-1} \times \frac{E - E_i}{E}, \quad i = 1,2,\cdots n, \tag{6}$$

E. Weight Function Distribution and Model Establishment of Nondestructive Detection Combined Prediction

In Table II, according to the calculated results of stress wave and impedance instrument for different kinds of woods and defects areas, combined predictive value can be obtained. For example, with XYS-1 the combined predictive overall value resulted from equation (3) was:

E=(21+31.57)/2=26.29cm2.

In the light of the definition of the Shapley Value, the 'cooperation relationship' members participating in the combined predicted model overall value distribution are: I={1,2} and its subset errors E{1}, E{2}, and E{1,2}. Their numerical value is the average value of the absolute value of subset error, namely 21 cm2, 31.57 cm2, and 26.29cm2.

According to equation (4) and (5), XYS-1 stress wave nondestructive detection Shapley value is:

$$E_1 = \frac{1! \times 0!}{2!}\left[E\{1\} - E(\{1\} - \{1\})\right] + \frac{0! \times 1!}{2!}\left[E\{1,2\} - E\{1,2\} - E\{1\}\right]$$

$$= \frac{1}{2}(21) + \frac{1}{2}(26.29 - 31.57) \ = \ 7.86 cm^2$$

Equally, specimen BYS-1 impedance instrument detection shared error value was: E2=18.43cm2. However, E1+E2=26.29cm2, which showed that the sum of the shared value of single detection method of stress wave and impedance instrument amounts to E. The magnitude of shared value reflects the precision of every testing method. In combined model, the ultimate weight function formula (6) of every single test is:

$$w_{a1} = \frac{1}{1-1} \times \frac{26.29 - 7.86}{26.29} = 0.70$$

$$w_{a2} = \frac{1}{1-1} \times \frac{26.29 - 18.43}{26.29} = 0.30$$

The Specimen XYS-1 two nondestructive testing methods combined model shared weight function was wa1=0.70 and wa2=0.30. In a similar way, the Specimen XYS-4 two nondestructive testing methods combined model shared weight function was wb1=0.56, and wb2=0.44; XYM-1 was wc1=0.53 and wc2=0.47; and XYM-4 was wd1=0.42 and wd2=0.58.

In accordance with the combined model shared weight function value as well as formula (2) of the two nondestructive testing methods for the above specimen, the combined model is:

Specimen XYS-1 internal defect model:
ft1=0.70×S1(XYS-1)＋0.30×S2(XYS-1);

Specimen XYS-4 internal defect model:
ft2=0.56×S1(XYS-4)＋0.44×S2(XYS-4);

Specimen XYM-1 internal defect model:
ft3=0.53×S1(XYM-1)＋0.47×S2(XYM-1);

Specimen XYM-4 internal defect model:
ft4=0.42×S1 (XYM-4)＋0.58×S2 (XYM-4).

The combined prediction models, in accordance to every specimen's stress wave and impedance instrument testing result, were recombined to predict the internal defect area. Therefore, achieving wood internal defect area (S3) and its relative error (Q3) is calculated (Table 2).

From Table 2, it is known that the average relative error of combined prediction models, on the basis of the Shapley value, is less than10%. Also, the average value of the absolute value of combined prediction internal defect is ordinarily smaller than that of the single testing error value by stress wave or impedance instrument.

IV. CONCLUSION

1. When wood internal defect is holes, stress wave is insensitive to smaller defects data collection and the defects boundaries are blurred. Wood internal defect shapes and positions can be quickly obtained by stress wave. When insects cause wood internal defect, internal complication of fiber damage renders S0 proportional to M1.

2. Impedance instrument two-dimensional plane detection figure can accurately determine wood internal defect positions as well as their types (holes/moth-eaten), but the results are only the single path of testing section. The internal defect of the whole section cannot be directly judged so well. The smaller the wood internal defects, the more precise the test results.

3. The Shapley value weight function distribution method is applied to decide the weight function of the results of wood internal tests launched by stress wave and impedance instrument. The average relative error is less than 10% and the testing accuracy of constructed combined predicted model is higher than that of single test results. Combined prediction provides not only favorable statistics for ancient buildings internal safety assessment, but also support for wood-health assessment.

CONFLICT OF INTEREST

The authors confirm that this article content has no conflicts of interest.

ACKNOWLEDGMENT

The authors are grateful for the support of the National Natural Science Foundation of China (51278003), the National Key Technology Support Program of China (2013BAK01B03), the Natural Science Foundation of Beijing, China (8132009), and the Foundation of Beijing University of Technology, China (ykj-2014-10666).

REFERENCES

[1] Q. Xie, P. zheng. W. Xiangi, et al. "Experimental study on seismic behavior of damaged straight mortise-tenon joints of ancient timber buildings,"Journal of Building Structures , vol.35, PP. 143-150, November 2014.

[2] Y. Pan, C. Wang, L. Tang, et al. "Study on mechanical model of straighi-tenon joints in ancient timber structures," Engineering Mechanics, vol.32, PP.82-89, February 2015.

[3] B. Ma. Wood Construction Techniques of Ancient Chinese Architecture, Science Press, Beijing, China, 2003.

[4] J. Vcelak, P. Kuklik, R. Zeleny, et al. "Optical fiber sensor for timber structure monitoring," Applied Mechanics and Materials, vol.827, pp.344-347, February, 2016.

[5] R. Lesko, M. Lopusniak. "Determination of Fire Resistance of Ceiling Structure Variant Design on the Basis of Timber Using Numerical Calculation Methods," Applied Mechanics and Materials, vol.820, pp. 379-384, January ,2016.

[6] J. Zhang, Q. Xu, Y. Xu, et al. “Research on residual bending capacities of used wood members based on the correlation between non-destructive testing results and the mechanical properties of wood,” Journal of Zhejiang University-Science A(Applied Physics and Engineering), vol.16, pp.541-550, July, 2015.

[7] X. Guo, S. Xu, X. Song, et al. “Safety assessment of ancient timber buildings based on gray-fuzzy analytical method,” Journal of Beijing University of Technology, vol.42, pp.393-398, March, 2016.

[8] K.Steppe, V.Cnudde, C. Girard, et al. “Use of X-ray computed microtomography for non-invasive determination of wood anatomical characteristics,” Journal of Structural Biology, vol.148, pp.11-21, October, 2004.

[9] A. Bastani, S.Adamopoulos, T. Koddenberg, et al. “Study of adhesive bondlines in modified wood with fluorescence microscopy and X-ray micro-computed tomography,” International Journal of Adhesion & Adhesives, vol.68, pp.351-358, July, 2016.

[10] G .Li, X. Weng, X.Du, X. Wang, et al. “Stress wave velocity patterns in the longitudinal–radial plane of trees for defect diagnosis” Computers & Electronics in Agriculture, vol.124, pp.23-28, March, 2016.

[11] T.Souza, E.Contado, R. Braga, et al. “Non-destructive technology associating PIV and Sunset laser to create wood deformation maps and predict failure,” Biosystems Engineering, vol.126, pp.109-116, Octobe, 2014.

[12] X. Ge, L.Wang, T.Sun, et al. “Quantitative detection of Salix matsudana inner decay based on stress wave and resistograph techniques,” China Forestry Science and Technology, vol.28, pp.87-91, May, 2014.

[13] H. Xu, L.Wang. “Effects of Cavity on Propagation Path of Stress Wave in Wood,”Journal of Northeast Forestry University, vol.42, pp.82-88, April, 2014.

[14] R. Flores, E. Molina, J. Tejada. “Assessment of groups in a network organization based on the Shapley group value,” Decision Support Systems, vol.83, pp.97-105, January, 2016.

[15] A. Ehsan, A. S.M.M, A. Hossein, et al. “Stochastic LMP (Locational marginal price) calculation method in distribution systems to minimize loss and emission based on Shapley value and two-point estimate method,”Energy, vol.107, pp.396-408, July , 2016.

[16] G. Zhang, G. Li, J. Li, et al. “Stress wave propagation time estimation algorithm for nondestructive testing of wood,” Journal of Zhejiang A＆F University, vol.31, pp.394-398, March , 2014.